View metadata, citation and similar papers at core.ac.uk

brought to you by CORE

provided by White Rose Research Online

This is a repository copy of *Random lasing in uniform perovskite thin films*.

White Rose Research Online URL for this paper:
https://eprints.whiterose.ac.uk/129965/

Version: Published Version

Article:
Safdar, Amna, Wang, Yue orcid.org/0000-0002-2482-005X and Krauss, Thomas F. orcid.org/0000-0003-4367-6601 (2018) Random lasing in uniform perovskite thin films. Optics Express. A75-A84. ISSN 1094-4087

https://doi.org/10.1364/OE.26.000A75

Reuse
Items deposited in White Rose Research Online are protected by copyright, with all rights reserved unless indicated otherwise. They may be downloaded and/or printed for private study, or other acts as permitted by national copyright laws. The publisher or other rights holders may allow further reproduction and re-use of the full text version. This is indicated by the licence information on the White Rose Research Online record for the item.

Takedown
If you consider content in White Rose Research Online to be in breach of UK law, please notify us by emailing eprints@whiterose.ac.uk including the URL of the record and the reason for the withdrawal request.

eprints@whiterose.ac.uk
https://eprints.whiterose.ac.uk/

Research Article | Vol. 26, No. 2 | 22 Jan 2018 | OPTICS EXPRESS A75
Optics EXPRESS

Random lasing in uniform perovskite thin films

AMMA SAFDAR, YUE WANG,* AND THOMAS F. KRAUSS

Department of Physics, University of York, York, YO10 5DD, UK
**yue.wang@york.ac.uk*

Abstract: Following the very promising results obtained by the solar cell community, metal halide perovskite materials are increasingly attracting the attention of other optoelectronics researchers, especially for light emission applications. Lasing with both engineered and self-assembled resonator structures, such as microcrystal networks, has now been successfully observed, with the low cost and the simple solution-based process being a particular attraction. The ultimate in simplicity, however, would be to observe lasing from a continuous thin film, which has not been reported yet. Here, we show random lasing action from such a simple perovskite layer. Our lasers work at room temperature; they are deposited on unpatterned glass substrates and they exhibit a minimum threshold value of 10 μJ/cm^2. By carefully controlling the solution processing conditions, we can determine whether random lasing occurs or not, using identical precursors. A rather special feature is that some of the films exhibit single and dual mode lasing action, which is rarely observed in random lasers. Our work fully exploits the simplicity of the solution-based process and thereby adds an important capability into the emerging field of perovskite-based light emitters.

© 2017 Optical Society of America

OCIS codes: (140.3490) Lasers, distributed-feedback; (250.0250) Optoelectronics; (310.0310) Thin films.

References and links

1. L. Protesescu, S. Yakunin, M. I. Bodnarchuk, F. Krieg, R. Caputo, C. H. Hendon, R. X. Yang, A. Walsh, and M. V. Kovalenko, "Nanocrystals of Cesium Lead Halide Perovskites ($CsPbX_3$, X = Cl, Br, and I): Novel Optoelectronic Materials Showing Bright Emission with Wide Color Gamut," Nano Lett. **15**(6), 3692–3696 (2015).
2. Z. K. Tan, R. S. Moghaddam, M. L. Lai, P. Docampo, R. Higler, F. Deschler, M. Price, A. Sadhanala, L. M. Pazos, D. Credgington, F. Hanusch, T. Bein, H. J. Snaith, and R. H. Friend, "Bright light-emitting diodes based on organometal halide perovskite," Nat. Nanotechnol. **9**(9), 687–692 (2014).
3. G. Xing, N. Mathews, S. S. Lim, N. Yantara, X. Liu, D. Sabba, M. Grätzel, S. Mhaisalkar, and T. C. Sum, "Low-temperature solution-processed wavelength-tunable perovskites for lasing," Nat. Mater. **13**(5), 476–480 (2014).
4. L. Etgar, P. Gao, Z. Xue, Q. Peng, A. K. Chandiran, B. Liu, M. K. Nazeeruddin, and M. Grätzel, "Mesoscopic $CH_3NH_3PbI_3/TiO_2$ Heterojunction Solar Cells," J. Am. Chem. Soc. **134**(42), 17396–17399 (2012).
5. J. Burschka, N. Pellet, S. J. Moon, R. Humphry-Baker, P. Gao, M. K. Nazeeruddin, and M. Grätzel, "Sequential deposition as a route to high-performance perovskite-sensitized solar cells," Nature **499**(7458), 316–319 (2013).
6. C. Motta, F. El-Mellouhi, and S. Sanvito, "Charge carrier mobility in hybrid halide perovskites," Sci. Rep. **5**, 12746 (2015).
7. T. S. Kao, Y. H. Chou, C. H. Chou, F. C. Chen, and T. C. Lu, "Lasing behaviors upon phase transition in solution-processed perovskite thin films," Appl. Phys. Lett. **105**, 231108 (2014).
8. P. Docampo and T. Bein, "A Long-Term View on Perovskite Optoelectronics," Acc. Chem. Res. **49**(2), 339–346 (2016).
9. S. D. Stranks and H. J. Snaith, "Metal-halide perovskites for photovoltaic and light-emitting devices," Nat. Nanotechnol. **10**(5), 391–402 (2015).
10. Y. Tian, A. Merdasa, E. Unger, M. Abdellah, K. Zheng, S. McKibbin, A. Mikkelsen, T. Pullerits, A. Yartsev, V. Sundström, and I. G. Scheblykin, "Enhanced Organo-Metal Halide Perovskite Photoluminescence from Nanosized Defect-Free Crystallites and Emitting Sites," J. Phys. Chem. Lett. **6**(20), 4171–4177 (2015).
11. S. Yakunin, L. Protesescu, F. Krieg, M. I. Bodnarchuk, G. Nedelcu, M. Humer, G. De Luca, M. Fiebig, W. Heiss, and M. V. Kovalenko, "Low-threshold amplified spontaneous emission and lasing from colloidal nanocrystals of caesium lead halide perovskites," Nat. Commun. **6**, 8056–8064 (2015).
12. J. Xing, F. Yan, Y. Zhao, S. Chen, H. Yu, Q. Zhang, R. Zeng, H. V. Demir, X. Sun, A. Huan, and Q. Xiong, "High-Efficiency Light-Emitting Diodes of Organometal Halide Perovskite Amorphous Nanoparticles," ACS Nano **10**(7), 6623–6630 (2016).

#305129 https://doi.org/10.1364/OE.26.000A75
Journal © 2018 Received 1 Sep 2017; revised 21 Oct 2017; accepted 2 Nov 2017; published 11 Dec 2017

Optics EXPRESS

13. N. Yantara, S. Bhaumik, F. Yan, D. Sabba, H. A. Dewi, N. Mathews, P. P. Boix, H. V. Demir, and S. Mhaisalkar, "Inorganic Halide Perovskites for Efficient Light-Emitting Diodes," J. Phys. Chem. Lett. **6**(21), 4360–4364 (2015).
14. R. Dhanker, A. N. Brigeman, A. V. Larsen, R. J. Stewart, J. B. Asbury, and N. C. Giebink, "Random lasing in organo-lead halide perovskite microcrystal networks," Appl. Phys. Lett. **105**, 151112 (2014).
15. F. Deschler, M. Price, S. Pathak, L. E. Klintberg, D. D. Jarausch, R. Higler, S. Hüttner, T. Leijtens, S. D. Stranks, H. J. Snaith, M. Atatüre, R. T. Phillips, and R. H. Friend, "High photoluminescence efficiency and optically pumped lasing in solution-processed mixed halide perovskite semiconductors," J. Phys. Chem. Lett. **5**(8), 1421–1426 (2014).
16. Q. Zhang, S. T. Ha, X. Liu, T. C. Sum, and Q. Xiong, "Room-Temperature Near-Infrared High-Q Perovskite Whispering-Gallery Planar Nanolasers," Nano Lett. **14**(10), 5995–6001 (2014).
17. H. Zhu, Y. Fu, F. Meng, X. Wu, Z. Gong, Q. Ding, M. V. Gustafsson, M. T. Trinh, S. Jin, and X. Y. Zhu, "Lead halide perovskite nanowire lasers with low lasing thresholds and high quality factors," Nat. Mater. **14**(6), 636–642 (2015).
18. G. L. Whitworth, J. R. Harwell, D. N. Miller, G. J. Hedley, W. Zhang, H. J. Snaith, G. A. Turnbull, and I. D. W. Samuel, "Nanoimprinted distributed feedback lasers of solution processed hybrid perovskites," Opt. Express **24**(21), 23677–23684 (2016).
19. Y. Jia, R. A. Kerner, A. J. Grede, A. N. Brigeman, B. P. Rand, and N. C. Giebink, "Diode-Pumped Organo-Lead Halide Perovskite Lasing in a Metal-Clad Distributed Feedback Resonator," Nano Lett. **16**(7), 4624–4629 (2016).
20. P. Brenner, M. Stulz, D. Kapp, T. Abzieher, U. W. Paetzold, A. Quintilla, A. Ian, H. Kalt, U. Lemmer, P. Brenner, M. Stulz, D. Kapp, and T. Abzieher, "Highly stable solution processed metal-halide perovskite lasers on nanoimprinted distributed feedback structures," Appl. Phys. Lett. **109**, 141106 (2016).
21. M. Saliba, S. M. Wood, J. B. Patel, P. K. Nayak, J. Huang, J. A. Alexander-Webber, B. Wenger, S. D. Stranks, M. T. Hörantner, J. T. W. Wang, R. J. Nicholas, L. M. Herz, M. B. Johnston, S. M. Morris, H. J. Snaith, and M. K. Riede, "Structured Organic-Inorganic Perovskite toward a Distributed Feedback Laser," Adv. Mater. **28**(5), 923–929 (2016).
22. S. A. Veldhuis, P. P. Boix, N. Yantara, M. Li, T. C. Sum, N. Mathews, and S. G. Mhaisalkar, "Perovskite Materials for Light-Emitting Diodes and Lasers," Adv. Mater. **28**(32), 6804–6834 (2016).
23. N. Pourdavoud, S. Wang, A. Mayer, T. Hu, Y. Chen, A. Marianovich, W. Kowalsky, R. Heiderhoff, H. C. Scheer, and T. Riedl, "Photonic Nanostructures Patterned by Thermal Nanoimprint Directly into Organo-Metal Halide Perovskites," Adv. Mater. **29**(12), 1605003 (2017).
24. Y. Zhou, M. Yang, W. Wu, A. L. Vasiliev, K. Zhu, and N. P. Padture, "Room-Temperature Crystallization of Hybrid-Perovskite Thin Films via Solvent-Solvent Extraction for High-Performance Solar Cells," J. Mater. Chem. A Mater. Energy Sustain. **3**, 8178–8184 (2015).
25. Z. Xiao, C. Bi, Y. Shao, Q. Dong, Q. Wang, Y. Yuan, C. Wang, Y. Gao, and J. Huang, "Efficient, high yield perovskite photovoltaic devices grown by interdiffusion of solution-processed precursor stacking layers," Energy Environ. Sci. **7**(8), 2619 (2014).
26. C. Chiang, Z. Tseng, and C.-G. Wu, "Planar heterojunction perovskite/$PC_{71}BM$ solar cells with enhanced open-circuit voltage via a (2/1)-step spin-coating process," J. Mater. Chem. A Mater. Energy Sustain. **2**, 15897–15903 (2014).
27. T. Baikie, Y. Fang, J. M. Kadro, M. Schreyer, F. Wei, S. G. Mhaisalkar, M. Graetzeld, and T. J. White, "Synthesis and crystal chemistry of the hybrid perovskite $(CH_3NH_3)PbI_3$ for solid-state sensitised solar cell applications," J. Mater. Chem. A Mater. Energy Sustain. **1**, 5628–5641 (2013).
28. H. Tsai, W. Nie, J.-C. Blancon, C. C. Stoumpos, R. Asadpour, B. Harutyunyan, A. J. Neukirch, R. Verduzco, J. J. Crochet, S. Tretiak, L. Pedesseau, J. Even, M. A. Alam, G. Gupta, J. Lou, P. M. Ajayan, M. J. Bedzyk, and M. G. Kanatzidis, "High-efficiency two-dimensional Ruddlesden-Popper perovskite solar cells," Nature **536**(7616), 312–316 (2016).
29. X. Zhao, Z. Wu, S. Ning, S. Liang, D. Wang, and X. Hou, "Random lasing from granular surface of waveguide with blends of PS and PMMA," Opt. Express **19**(17), 16126–16131 (2011).
30. D. Wiersma, "Light in strongly scattering and amplifying random media," (1995).
31. S. F. Yu, C. Yuen, S. P. Lau, W. I. Park, and G. C. Yi, "Random laser action in ZnO nanorod arrays embedded in ZnO epilayers," Appl. Phys. Lett. **84**(17), 3241–3243 (2004).
32. H. Cao, Y. G. Zhao, S. T. Ho, E. W. Seelig, Q. H. Wang, and R. P. H. Chang, "Random laser action in semiconductor powder," Phys. Rev. Lett. **82**(11), 2278–2281 (1999).
33. H. Cao, J. Y. Xu, Y. Ling, A. L. Burin, E. W. Seeling, X. Liu, and R. P. H. Chang, "Random Lasers with Coherent Feedback," IEEE J. Sel. Top. Quantum Electron. **9**(1), 111–119 (2003).
34. Y. Wang, G. Tsiminis, Y. Yang, A. Ruseckas, and A. L. Kanibolotsky, "Broadly tunable deep blue laser based on a star-shaped oligofluorene truxene," Synth. Met. **160**, 1397–1400 (2010).
35. L. Qin, L. Lv, Y. Ning, C. Li, Q. Lu, L. Zhu, Y. Hu, Z. Lou, F. Teng, and Y. Hou, "Enhanced amplified spontaneous emission from morphology-controlled organic-inorganic halide perovskite films," RSC Advances **5**, 103674 (2015).

Optics EXPRESS

1. Introduction

The family of metal halide perovskite materials has recently caused a step-change in the photovoltaics community based on their efficient absorption properties and the high open-circuit voltages they provide. Motivated by these excellent optoelectronic properties, researchers have in turn also examined their light emission properties and have reported LED [1,2] and lasing operation [3] over a broad wavelength range. Processing flexibility, simplicity and low-cost precursor materials are major drivers with a view towards ultra-low-cost applications, such as wearable electronics or single-use devices for medical diagnostics or therapeutics. The ultimate in simplicity for a laser device, naturally, is a laser that creates its own feedback through scattering in the gain medium, i.e. a random laser. Here, we demonstrate how such a random laser can be created by simply controlling the solution-processing conditions of the perovskite material. It is now well established that the family of lead triiodides, i.e. materials with the PbI_3 ion at the core of its crystal unit cell and a bandgap around 1.6 eV, forms the most efficient and stable material for optoelectronic applications [4,5]. An approximately 500 nm thick film of this material is sufficient to absorb light over the entire visible spectrum, with very low sub-gap absorption. Bipolar charge is transported in solid-state films with good ambipolar charge carrier mobility ($5 - 10\,cm^2V^{-1}s^{-1}$ for electrons and $1 - 5\,cm^2V^{-1}s^{-1}$ for hole carriers [6,7], long carrier lifetime (10 ns) and sufficiently large diffusion length (micrometer-scale) [8], which leads to low non-radiative recombination in the bulk [9]. The perovskite material family also provides attractive optoelectronic properties, including strong photopumped light emission [10,11], bright electroluminescence [12,13], and the observation of optically pumped lasing, along with wide wavelength tuneability [1,14,15].

The laser configurations demonstrated so far include triangular or hexagonal platelet structures utilising whispering gallery modes (WGM) [16] or planar wire configurations that form Fabry-Perot cavities [17]. Similarly, self-organised microcrystalline rod-shaped structures have been used as resonators [14]. Perovskite distributed feedback (DFB) lasers have also been studied recently, with gratings made by electron beam, UV and holographic lithography techniques [18–21]. Typical thresholds are in the 100 $\mu J/cm^2$ regime [22]. The reason for the moderate thresholds most likely arise from the surface roughness of perovskite thin films, which scatter the laser mode in the DFB resonators, leading to high losses. Lower threshold thin film perovskite DFB lasers have been recently demonstrated in a 2D photonic crystal laser (threshold of 3.8 $\mu J/cm^2$), which can be obtained by patterning and flattening the perovskite layer with a thermal nanoimprint process [23].

All of these observations require carefully engineered nanostructures, the addition of external layers or very controlled crystal growth conditions to achieve a desired configuration that can act as a laser resonator. In order to meet the requirements of a true low-cost technology, it would be preferable to keep the process steps as simple as possible. Here, we show a possible route towards such an inexpensive technology by demonstrating high-performance random lasing from a uniform perovskite film. We study perovskite materials of the methylammonium lead triiodode ($CH_3NH_3PbI_3$) family by investigating systematically the conditions required for achieving (and avoiding) random lasing and using optical gain and loss measurements to explain the different operating regimes. The low thresholds we obtain ($\approx$10 $\mu J/cm^2$), i.e. lower than for many of the engineered feedback structures mentioned above, indicate that the roughness of the perovskite thin film naturally offers itself for random lasing.

2. Fabrication

We use the synthesis method reported by Zhou et al [24] to produce the thin films on glass substrates. Thin films are the key to achieving the strong optical confinement and the high charge carrier densities required for high luminescence efficiency. The method consists of a

Optics EXPRESS

single-solution deposition step by spin-coating followed by an anti-solvent dip step for drying of the film. A single precursor solution of lead iodide (PbI_2) and methylammonium iodide (CH_3NH_3I), mixed in a 1:1 molar ratio, is prepared in N-Methyl-2-pyrrolidone (NMP) solvent. The concentrations of the precursor solutions are kept at 1M to obtain the desired film thickness and good surface coverage. The solution is spin-coated on to the glass substrate (1.5 x 1.5 mm^2) and the solvent is then extracted by dipping the sample in a diethyl ether (DEE) bath, without any need for a high-temperature annealing step. The appearance of the final perovskite film is both uniform and shiny. The film thickness and quality are well controlled by varying two parameters: (a) spin speed and (b) dip time in anti-solvent. The dip time is an extremely important parameter here as it significantly affects the crystallization of the film. We note that by increasing the dip time from 0 to 120 seconds, we can achieve better coverage on the glass surface, which is a primary challenge in the synthesis of thin perovskite films. We also observe that the dip time is particularly critical at determining the difference between lasing and no-lasing action.

An alternative method described in the literature for achieving high quality perovskite films is the double deposition solution (DDS) method [25,26]. The DDS method consists of first spin-coating a layer of PbI_2 from a 0.5 M solution in dimethylformamide (DMF) and then annealing at 70 °C for 30 minutes. Once the film is dry, it is dipped into a solution of CH_3NH_3I (10 mg/ml) in 2-propanol (IPA) for 20 seconds, followed by a final annealing at 100 °C for 1 hour.

The films were physically characterised by scanning electron microscope (SEM) and X-ray diffraction (XRD). The optical characterisation consists of photoluminescence (PL) measurements as well as gain and loss measurements, all performed with a pulsed frequency doubled YAG laser (pulse length of 400 ps, repetition rate of 500 Hz) at 532 nm (PhotonicSolutions PowerChip NanoLaser). The pump intensity incident on the samples was controlled by a selection of calibrated neutral density filters. The excitation energy was measured with a ThorLABs powermeter (PM100D).

3. Results

We performed a wide-ranging parameter scan of molar concentration, substrate preparation (for uniform coverage), spin speed (for film thickness) and solvent extraction time (for crystalisation). We found four methods that best represent the dominant trends we observe and refer to them as Methods A, B1, B2 and B3, as detailed in Table 1. It is worth noting here that the cut-off thickness of fundamental modes in an air-$CH_3NH_3PbI_3$-glass waveguide is calculated to be much less than 50 nm, while the films that are thicker than 80 nm can support more than one mode.

Table 1. Synthesis parameters for the four methods illustrated in Figs. 1 and 2.

Method ID	Precursor solvent	Deposition method	Dip time /sec	Spin speed /rpm	Annealing time /min	Average film thickness /nm	Roughness R_{rms} /nm
Method A	Dimethylfo-rmamide	Double step	N/A	2000	60 @100 °C	275	80
Method B1	N-Methyl-2-pyrrolidone	Single step	0	2000	0	230	18
Method B2	N-Methyl-2-pyrrolidone	Single step	3	2000	0	81	24
Method B3	N-Methyl-2-pyrrolidone	Single step	120	2000	0	56	26

Optics EXPRESS

A comparison of the photoluminescence behaviour of the four methods, together with their surface morphology, is shown in Figs. 1 and 2. Films produced by Methods A and B1 only show photoluminescence, while Methods B2 and B3 films exhibit lasing/multimode lasing, all using the same excitation energy of 212 μJ/cm^2. From the SEM images, we see that Method A produces films with grains of large size (~500 nm), while Method B1 produces very smooth films and Method B2 and B3 produce films of intermediate roughness. The root mean square (rms) roughness values (R_{rms}) given in Table 1 are measured with Atomic Force Microscopy, see Figs. 2(e)-2(h). We have obtained very uniform surface coverage of our thin films on glass substrates, evidenced in Fig. 2(i)-2(j), the cross-sectional SEM images of films produced by Method A and Method B3 for instance. The existence of a crystalline phase is indicated by indexed X-ray diffraction patterns as shown in Fig. 3. The X-ray analysis confirms that all four methods produce perovskite crystals [27]. The 14.1°, 24.4° and 28.4° diffraction peaks are associated with the (110), (202) and (220) planes of the tetragonal phase of $CH_3NH_3PbI_3$ perovskite.

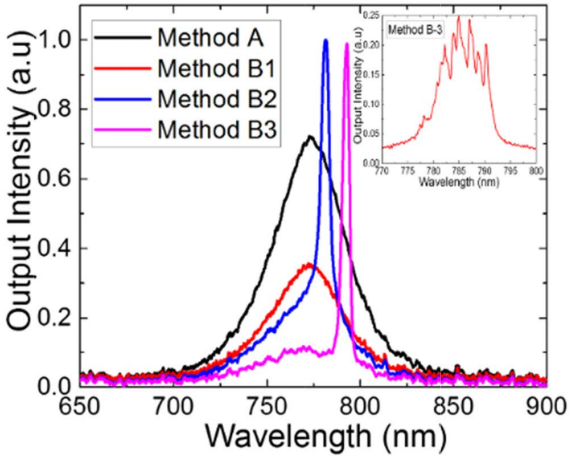

Fig. 1. Output emission spectra of perovskite films produced by the four methods, collected at an excitation energy of 212 μJ/cm^2. The inset shows multimode lasing observed for a higher resolution scan with a film prepared using Method B3.

Optics EXPRESS

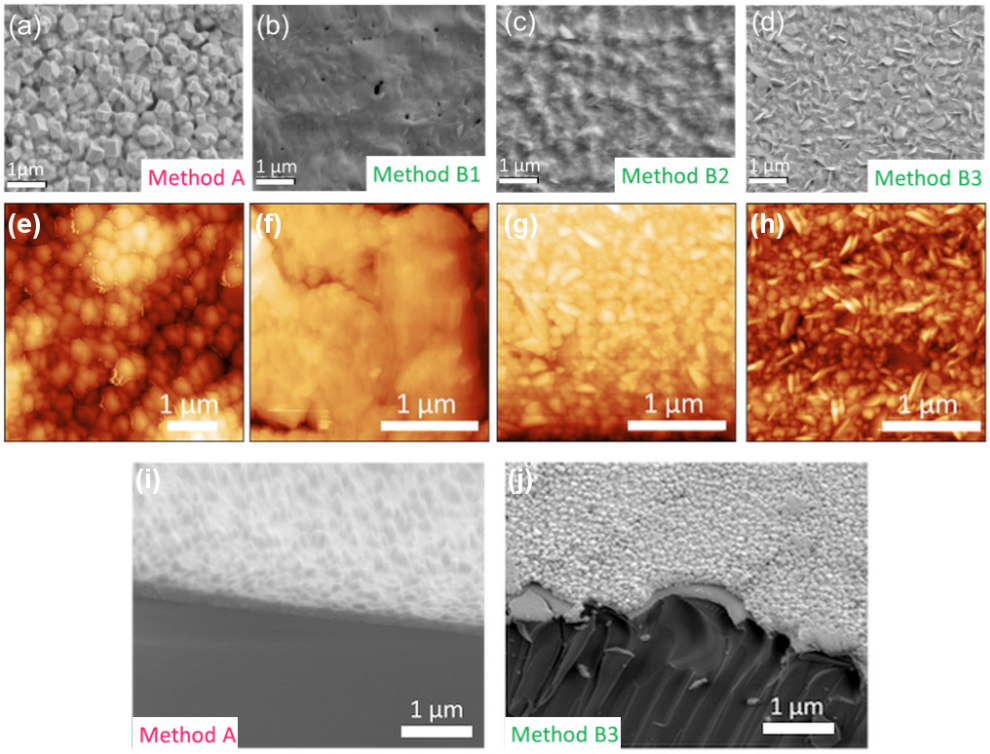

Fig. 2. Morphology comparison for four different fabrication methods. (a): SEM image of perovskite film synthesized by the double deposition step method (Method A). (b): SEM image of perovskite film synthesized via solvent extraction method with 0 sec dip time (Method B1). (c) and (d): SEM images of perovskite films synthesized via solvent extraction method with 3 second (Method B2) and 120 second (Method B3) dip time; (e-h): AFM images of films produced by Method A, B1, B2 and B3; (i-j): cross-sectional SEM images of films produced by Method A and Method B3, viewed at an angle of 45°.

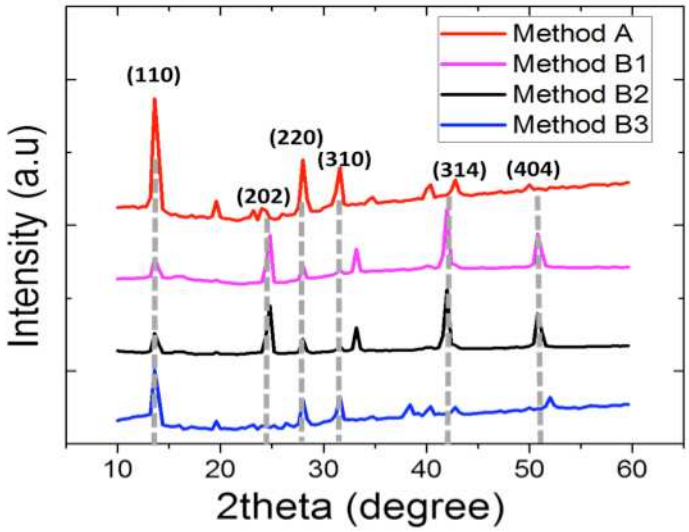

Fig. 3. X-ray diffraction patterns of tetragonal-phase iodide based perovskite films synthesized by four methods.

Optics EXPRESS

Next, we study the luminescence behaviour of the films in more detail, under pump intensities up to 100 μJ/cm^2. A lens was used to shape the excitation beam into a spot of 1.33 mm in diameter and the emission spectra were collected by a ThorLABs spectrometer (CCS175/M) at normal incidence. The difference between the films made by Method B1, B2 and B3 is particularly striking, as they only differ in a single fabrication parameter, namely the dip time in the anti-solvent. For Method B1, with 0 second dip time, we observe broadband photoluminescence for all pump intensities, which is typical for lead iodide perovskite films. The PL intensity increases linearly and the linewidth remains constant near 45 nm (FWHM). Further evidence for random lasing action is shown in Fig. 4 where we observe (a) single mode, (b) dual mode and (c) multimode lasing. The multimode lasing in Fig. 4(c) is commonly observed for random laser behaviour, while the single and dual mode lasing is rather unique. These spectra were taken for the same film made from Method B3 under a pump intensity of 13.4 μJ/cm^2 at different positions on the film.

Moreover, the lasing actions from the films prepared by Method B3 are further investigated with different pumping geometries, along with the amplified spontaneous emission (ASE). The dual mode lasing behaviour as a function of pump intensity, observed in Method B3, is shown in Figs. 5(a) and 5(c). Mode 1 and Mode 2 lasing occurs when the pump intensity is increased to 11 μJ/cm^2 and 13 μJ/cm^2 respectively, when the sample is excited with a circular beam with a diameter of 1.33 mm. These perovskite films are not encapsulated at all. We have observed the lasing threshold increased by approximately 20% after 48-hour exposure to air and light. For pumping at 500 Hz (17 μJ/cm^2) in air, the random laser output decreased to 80% of its initial value after 10^5 pulses as shown in Fig. 6. We note that with suitable encapsulation, much longer lifetimes of perovskite-based optoelectronic devices have already been observed [28].

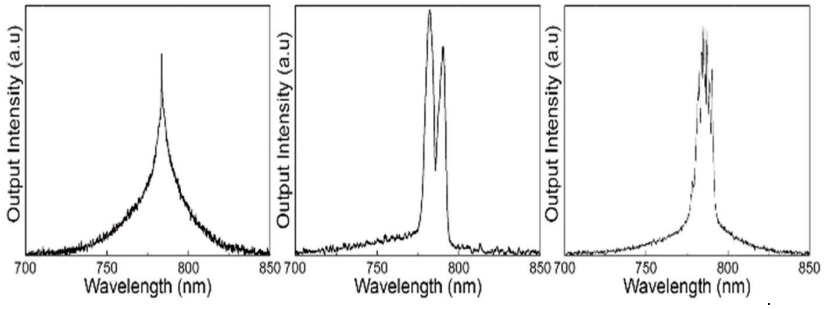

Fig. 4. Random lasing observed in a perovskite uniform thin film: (a) Single mode lasing; (b) Dual mode lasing; and (c) Multimode random lasing. All spectra were taken from the same film prepared by Method B3, under a fixed excitation intensity of 13.4 μJ/cm^2.

Optics EXPRESS

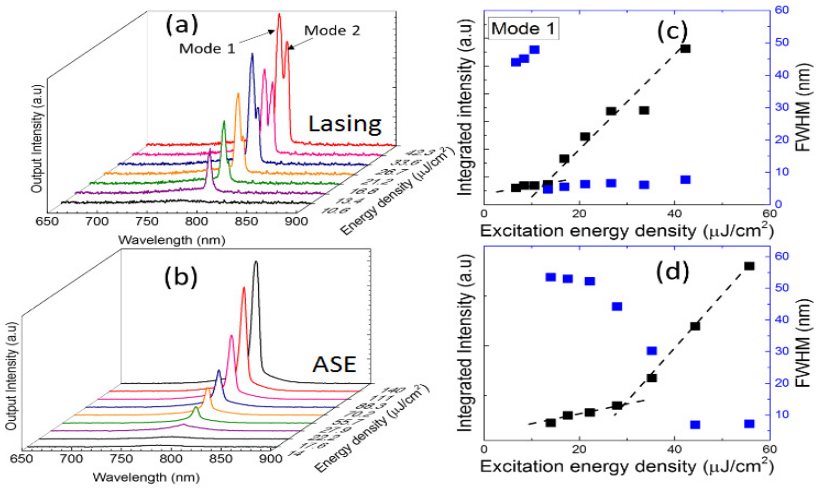

Fig. 5. All spectra collected are from Method B3 (120 sec) films. (a) Surface emission spectra for a film excited with a circular excitation spot with a diameter of 1.33 mm, with a laser threshold of 11 μJ/cm^2 shown in (c) along with its Full Width Half Maximum (FWHM); (b) Amplified spontaneous emission spectra of films excited with a narrow stripe in 1.6 x 0.4 mm^2 dimension and detected from the edge of the sample. The ASE threshold of 39 μJ/cm^2 is shown in (d).

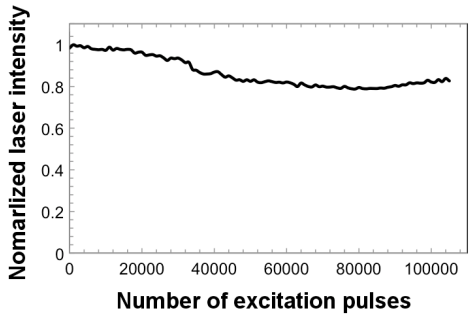

Fig. 6. Lasing stability of random laser for 500 Hz pumping rate.

In order to further verify that we are indeed observing lasing action, we also study the ASE, as ASE provides a similar step-change that can easily be mistaken for lasing. One typically expects the ASE threshold to be higher than the lasing threshold and its FWHM broader than the lasing peak. The presence of an ASE threshold also determines the film's compatibility as a gain medium and allows us to measure the gain and loss coefficients. For the ASE measurements, we follow the procedure commonly used for examine organic semiconducting gain materials [29], whereby we excited the film with a stripe-shaped beam in 1.6 x 0.4 mm^2 dimension and detect the emission from the edge of the film. The long axis of the beam is oriented perpendicular to the edge of the sample where the emission is monitored, thereby forming a gain-guide which transports the spontaneously emitted light to the edge of the film while getting amplified along the way. It is worth noting here that the emission spectrum collected from the surface of the films (at normal incidence) mainly exhibits random lasing, along with much lower intensity of background PL. In contrast, the spectrum detected from the edge of the thin film mainly consists of ASE. To evidence the difference between lasing and ASE, we measure an ASE threshold of 39 μJ/cm^2 for Method B3 (Figs. 5(b) and 5(d)), which is significantly higher than the lasing threshold of 12 μJ/cm^2 for the same film excited with the same stripe-shaped beam.

Optics EXPRESS

To understand the mechanism of the random lasing behaviour, we consider the interplay between gain and scattering. Random lasing can be understood as a random walk that forms an open [30] or a closed loop [31,32]. Alternatively, one can think of it as constructive interference between multiple scattering events, which is sharpened by the gain [33]. In either case, it is essential to have multiple scattering events N in the thin film, separated by the mean free path length $L_{scatter,}$ such that the total pathlength before the light is scattered out is longer than the gain length L_{gain}, i.e. $N L_{scatter} > L_{gain}$. If the scattering is too weak, N is too small even though $L_{scatter}$ may be large; on the other hand, if the scattering is too strong, the mean free path $L_{scatter}$ is too short and the light may be scattered out before experiencing significant gain; note that $L_{scatter}$ here refers to in-plane scattering. Therefore, it is essential that a certain amount of scattering occurs and that scattering and gain interplay correctly.

To determine the gain of the films, the variable stripe length method is used [34] whereby the output intensity, $I(\lambda)$ is related the gain coefficient of the material by following given relation:

$$I(\lambda) = \frac{AI_o}{g(\lambda)}(\exp^{g(\lambda)L} - 1), \tag{1}$$

where L is the length of the stripe incident on the film, A is a cross-section constant, I_o is the pump intensity and $g(\lambda)$ is the net gain coefficient of the material. We then use a log-linear plot for the experimental data and place a linear fit to extract the gain values for the three films made using Method A, B2 and B3 (see Fig. 7). The length of the excitation stripe is varied between 0 to 3 mm with an excitation energy density of 500 μJ/cm^2. The resulting gain values for Materials A, B2 and B3 are shown in Table 2. It is clear that the gain value is highest for Method B3, as expected from its low lasing threshold. The gain values of our films are comparable to other reported solution processed perovskite thin-films [35].

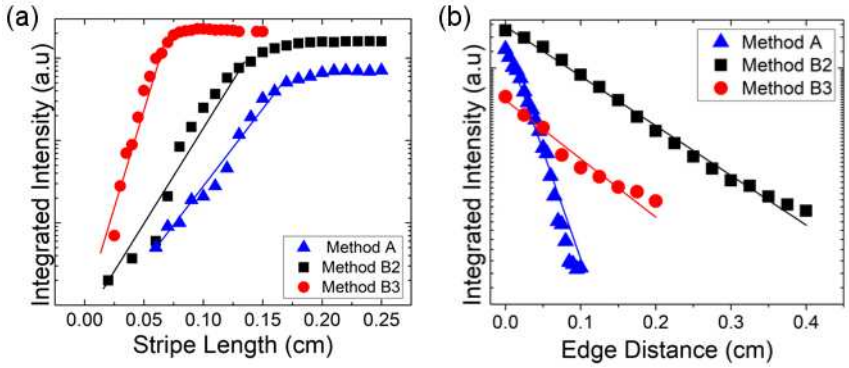

Fig. 7. (a) Variable stripe length method based measurements for gain coefficient in perovskite films; (b) output emission intensity as a function of un-pumped region distant from the edge of the sample to determine loss coefficients in samples prepared by Method A, B2 and B3.

For the loss coefficient measurements, a similar method is used, whereby the pumped length is held constant at 2 mm, and the stripe is moved away from the edge of the film to increase the un-pumped area where the amplified light travel through. The net loss then follows the simple Beer-Lambert law,

$$I = I_o e^{(-\alpha x)}, \tag{2}$$

where x is the distance between the film edge to the end of the stripe and α is the loss coefficient. Please note that this method measures the out-of-plane scattering loss including self-absorption loss. The experimental data is again plotted log-linearly. From the fit to the linear section of the graphs, we extract the loss values as shown in Table 2.

Optics EXPRESS

We can now provide a semi-quantitative explanation for the observed lasing/nonlasing phenomena. Intuitively, one would expect Material A to be the best candidate for random lasing, as the SEM image shows a very "blocky" appearance, which suggests strong scattering. Correspondingly, we measure a high scattering loss of 19.8 cm^{-1}. Nevertheless, as Material A exhibits less gain than Material B3, we conclude that the effective pathlength $NL_{scatter}$ is shorter than the gain length L_{gain}, so lasing does not occur. It may also be the case that the out-of-plane scattering component is too strong compared to the in-plane scattering component. For Material B1, the opposite is true: the scattering is weak and the gain is too low, which again precludes lasing. Materials B2 and B3, however, exhibit a good balance between gain and scattering such that the $NL_{scatter} > L_{gain}$ condition is met and lasing can occur.

Table 2. ASE threshold and the gain and loss coefficient values.

Method ID	ASE threshold /μJ/cm^2	Gain coefficient /cm^{-1}	Loss coefficient /cm^{-1}
Method A	415	28.9 ± 1.0	19.8 ± 1.0
Method B1	Not observed	Not applicable	Not applicable
Method B2	33	16.8 ± 1.5	2.9 ± 0.1
Method B3	39	70.1 ± 2.6	4.6 ± 0.3

4. Conclusions

In summary, we have found a simple room temperature method for depositing uniform perovskite films that exhibit random lasing action. The films show strong amplification as well as all the features expected from a random laser, e.g. nonlinear output curve, linewidth narrowing and ASE threshold for higher pump intensity. A rather special and rarely observed feature is that some of the films exhibit single and dual mode lasing action. We also show how to control the random lasing action by varying the dip time in the anti-solvent, as this step controls the nature of the film crystallization, which has a significant affect on optical gain, thereby determining the difference between lasing and no-lasing action.

Funding

Engineering and Physical Sciences Research Council (EPSRC) "Structured Light" Programme (EP/J01771X/1).

Acknowledgment

AS gratefully acknowledges PhD studentship awarded by National University of Sciences and Technology (NUST), Islamabad, Pakistan. We also acknowledge fruitful discussions on random lasers with Prof W Vos of University of Twente, The Netherlands.

144.32.225.77 {ts '2018-04-23 05:10:04'}